Supplementary Information

Materials and Methods

Purification and crystallization

The zebrafish VDR LBD (residues 156–453) was cloned as an N-terminal hexahistidine-tagged fusion protein in pET28b expression vector (Novagen) and overproduced in *Escherichia coli* BL21 (DE3) strain. Cells were grown at 37 °C for two hours and subsequently incubated for three hours at 25 °C with 1 mM isopropyl thio-β-D-galactoside. Protein purification included two successive chromatography steps, a metal affinity chromatography on a cobalt-chelating resin (Talon®, Clontech) and a gel filtration step on a size-exclusion chromatography Superdex S75 16/60 column (Pharmacia). The $(His)_6$-tag was removed by bovine thrombin digestion overnight at 4 °C between the two chromatography steps. The final buffer contained 10 mM Tris/HCl pH 7.5, 200 mM NaCl. 2 mM of TCEP was added in each fractions of interest. The protein was concentrated using Amicon ultra-30 (Millipore) to 3-7 mg/ml and incubated with a 1/100 v/v ratio of ligand and a three-fold excess of the coactivator GRIP1 peptide (686- KHKILHRLLQDSS-698). Crystals were obtained in the same condition as for the native zVDR LBD protein [26]. Reservoir solutions contained 50 mM Bis–Tris pH 6.5, 1.6 M lithium sulfate and 50 mM magnesium sulfate.

X-Ray data collection and structure determination

Protein crystals were mounted in fiber loop and flash-cooled under the nitrogen flux after cryo-protection with oil. Data collection from a single frozen crystal was performed at 100K at ESRF (Grenoble, France), beamline ID-14-1. Crystals belong to the hexagonal space group $P6_522$ with one monomer per asymmetric unit. Data were integrated and scaled using HKL2000 [27] (see statistics in Supplementary Table 1). Crystal structures of zVDR LBD

complexed to Gemini-0072 and to Gemini-0097 were solved using a rigid body refinement with the known zVDR LBD/gemini structure as a starting model and refined at 2.4 Å and 2.5 Å resolution, respectively. Alternate cycles of maximum likelihood refinement and model fitting were subsequently performed to generate the final models of the complexes. The programs, Phenix.refine [28] and Coot [29] were used throughout structure determination and refinement. In both zVDR LBD/Gemini-0072 and zVDR LBD/Gemini-0097 complexes, the ligand was only added at the last stage of refinement. The omit map from the refined atomic model was used to fit the ligand into its electron density. Anisotropic scaling, a bulk solvent correction and TLS restrains were used. Four TLS segments were generated with the program TLSMD [30]. Restrained atomic B-factors were refined isotropically. Solvent molecules were added according to unassigned peaks in the electron density map. The average temperature factors for the ligands (46.5 $Å^2$ and 55.5 $Å^2$ for Gemini-0072 and Gemini-0097, respectively) are lower than those for proteins (60.5 $Å^2$ and 65.6 $Å^2$ for zVDR LBD/Gemini-0072 and zVDR LBD/Gemini-0097 complexes, respectively). All data were included in the refinement (no δ cutoffs). The two refined models show unambiguous chirality for both ligands. According to Procheck [31], 97.9 % and 95.5 % of the protein lies in most favored regions for zVDR LBD/Gemini-0072 and zVDR LBD/Gemini-0097 complexes, respectively. The final models of zVDR LBD/Gemini-0072 and /Gemini-0097 complexes contained residues from 154 to 190 and from 250 to 453 with no electron density for insertion region 191-250. The volumes of each ligand binding pocket were calculated using the CASTp server (Computed Atlas of Surface of Topography of protein) [32] and volumes of each ligand were calculated using GRASP [33]. Crystallographic data are summarized in Supp. Table 1.

Protein expression Vectors

The chimera Gal4–zVDR LBD (156-453) was constructed by PCR using appropriate oligonucleotides with restriction sites (BamHI/BglII) and cloned into the vector PXJ440

encoding the DBD of the yeast activator Gal4 (1–147). For over-expression in *Escherichia coli*, the zVDR LBD was subcloned into the NdeI/BamHI sites of pET28b.

Transactivation

Luciferase reporter activity was determined by using luciferin as the substrate and and β-galactosidase activity was measured using ortho-nitrophenyl-β-galactoside as the substrate. The chemiluminescence from activated luciferin was measured on a luminometer plate reader LB96P (Berthold Technologies). Luciferase values were normalized to the β-galactosidase activity. Luciferase activities are expressed as arbitrary units of light intensity. Data points represent the mean of assays performed in triplicate for at least three independent experiments. For every triplicate, the mean and the standard deviation of the mean was calculated.

Steady-state fluorescence anisotropy measurements

Steady-state anisotropy measurements were performed with a T-format SLM 8000 spectrofluorometer. Anisotropy titrations were carried out by adding increasing zVDR LBD concentrations to 1 μM fluorescent labeled TAMRA (Tetramethylrhodamine)-SRC-1 peptide in 20 mM TRIS-HCl (pH 7.5), 200 mM NaCl. The sequence of the SRC-1 peptide was the following: RHKILHRLLQEGSPS. Binding affinity of the SRC-1 peptide to zVDR LBD was quantified in response to gemini, Gemini-0072 or Gemini-0097. The excitation wavelength was 550 nm and the emitted light was monitored through high-pass filters (550 nm) (Kodak). Assuming that zVDR binds with the TAMRA-SRC-1 peptide in a 1:1 stoechiometry, the model used to describe the binding experiment was the following:

$$R + L \xleftrightarrow{Kd} P$$

L and R represent the zVDR LBD and the TAMRA-SRC-1 peptide respectively and P designates the zVDR LBD/TAMRA-SRC-1 complex.

The Scatchard equation was rewritten to fit the anisotropy, r, as follows:

$$r = r_0 + (r_f - r_0)\left(\frac{(Rt + Lt + Kd) - \sqrt{(Rt + Lt + Kd)^2 - 4RtLt}}{2Rt}\right)$$

Lt and Rt are the total concentration of zVDR LBD and TAMRA-SRC-1 peptide, respectively; rf represents the anisotropy at the plateau when all the complex is formed, whereas r_0 and r correspond to the anisotropy values of TAMRA-SRC-1 peptide in the absence and in the presence of a given concentration of zVDR, respectively. kd corresponds to the dissociation constant of the complex. All experiments were performed at 20°C and results are representative of three distinct experiments.

Supplementary Table 1: Data collection and refinement statistics

	Gemini-0072	Gemini-0097
Data Processing		
Resolution (Å)	50.0-2.40 (2.49-2.40)	50.0-2.50 (2.59-2.50)
Crystal space group	$P6_522$	$P6_522$
Cell parameters (Å)	a=b=66.11 ; c=264.64	a=b=66.16 ; c=264.52
Unique reflections	13853 (1378)	12720(1225)
Mean redundancy	2.8	4.7
Rsym (%)*	5.8 (35.1)	11.0 (25.6)
Completeness (%)	96.2 (99)	98.7 (100)
Mean I/σ (%)	14.8 (2.3)	18.1 (13.9)
Refinement		
R.m.s.d. bond length (Å) ¶	0.005	0.011
R.m.s.d. bond angles (°)	1.049	1.432
Rcryst (%)§	19.8	20.0
Rfree (%)	26.5	26.8

Values in parentheses correspond to the highest resolution shell
*R_{sym} (I) = $\Sigma_{hkl}\ \Sigma_i\ |\ I_{hkl\ ,\ i} - < I_{hkl} >\ |\ /\ \Sigma_{hkl}\ \Sigma_i\ |\ I_{hkl\ ,\ i}\ |$ with $< I_{hkl} >$ the mean intensity of the multiple $I_{hkl\ ,\ i}$ observations for symmetry-related reflections.
¶Root-mean-squared deviation (R.m.s.d.) are given from ideal values.

§$R_{cryst} = \Sigma_{hkl} \mid F_{obs} - F_{calc} \mid / \Sigma_{hkl} \mid F_{obs} \mid$, where F_{obs} and F_{calc} are the observed and calculated structure amplitudes, respectively. R_{free} is the same as R_{cryst}, but calculated on the 10% of data excluded from refinement.

Supplementary Figure S1: Transient transfection assays were done with gal4-zebrafish VDR in response to 1α,25(OH)$_2$D$_3$, parental gemini, Gemini-0072 and Gemini-0097. of zVDR in MCF-7 cells were performed to determine the EC_{50} values. A sigmoidal dose response curve was used to calculate the EC_{50} values for the dose-response curves measuring transcriptional activities and using Origin 6.1 software. Data are mean values (± SD) from a representative experiment out of two independent studies, each done in triplicates.

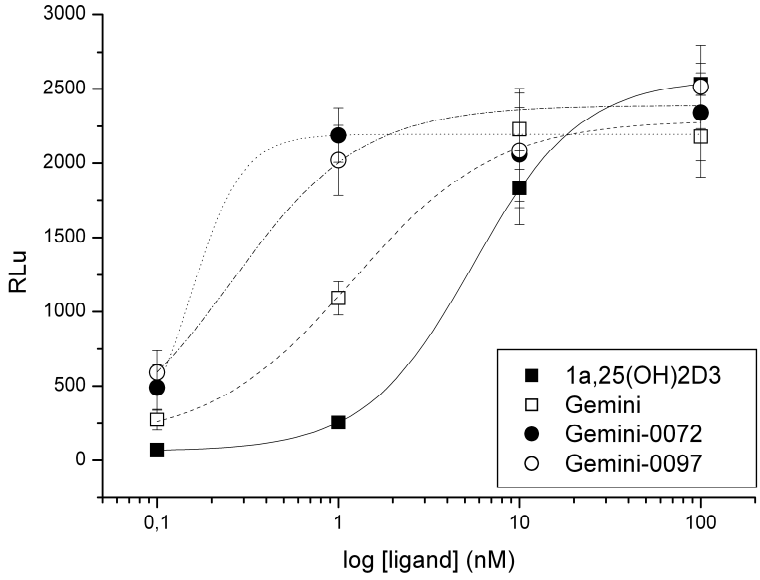

Supplementary Figure S2: Action of Gemini ligands on cell proliferation. MCF10AT1, MCF10DCIS AND MCF10CA1a cells were seeded on a 24-well plate (10,000 cells/well) and treated with compounds (0.01, 0.1, 1, 10 and 100 nM) in 5 % horse serum/DMEM/F12 media for 3 days. One μCi of [^{3}H]thymidine per well was added and the amount of incorporated radioactivity in DNA was measured using a liquid scintillation spectrometer. The experiment was repeated three times. The data are represented as mean ± standard deviation from three independent experiments. ●1α,25(OH)$_2$D$_3$, ▲Gemini-0072 and □ Gemini-0097.

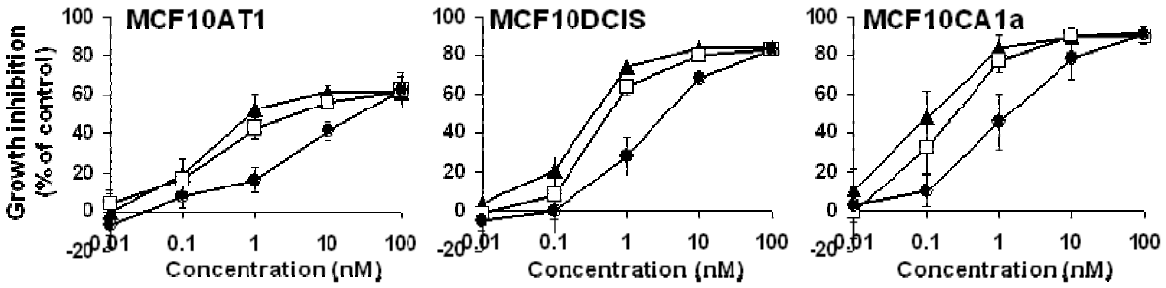

References

26. Ciesielski, F., Rochel, N. & Moras, D. Adaptability of the Vitamin D nuclear receptor to the synthetic ligand Gemini: remodelling the LBP with one side chain rotation *J. Steroid Biochem. Mol. Biol.* **2007** 103, 235-42

27. Otwinowski, Z. and Minor, W. (1997) Processing of X-ray diffraction data collected in oscillation mode. *Methods in Enzymology 276,* 307-326 Academic Press (New York).

28. Afonine, P.V., Grosse-Kunstleve, R.W. & Adams, P.D. A robust bulk-solvent correction and anisotropic scaling procedure *Acta Crystallogr. D Biol. Crystallogr.* **2005** 61, 850-5

29. Emsley, P. & Cowtan, K. Coot: model-building tools for molecular graphics *Acta Crystallogr. D Biol. Crystallogr.* **2004** 60, 2126-32

30. Painter, J. & Merritt, E.A. Optimal description of a protein structure in terms of multiple groups undergoing TLS motion *Acta Crystallogr. D Biol. Crystallogr.* **2006** 62, 439-50

31. Lovell, S.C., Davis, I.W., Arendall, W.B.3., de Bakker, P.I.W., Word, J.M., Prisant, M.G., Richardson, J.S. & Richardson, D.C. Structure validation by Calpha geometry: phi,psi and Cbeta deviation *Proteins* **2003** 50, 437-50

32. Dundas, J., Ouyang, Z., Tseng, J., Binkowski, A., Turpaz, Y. & Liang, J. CASTp: computed atlas of surface topography of proteins with structural and topographical mapping of functionally annotated residues *Nucleic Acids Res.* **2006** 34, W116-8

33. Nicholls, A., Sharp, K.A. & Honig, B. Protein folding and association: insights from the interfacial and thermodynamic properties of hydrocarbons *Proteins* **1991** 11, 281-96